Sulfate-Enhanced Catalytic Destruction of 1,1,1-Trichlorethane over Pt(111)

Adam F. Lee* and Karen Wilson

Department of Chemistry, University of York, York YO10 5DD, U.K.

Received: August 18, 2005; In Final Form: November 15, 2005

The catalytic destruction of 1,1,1-trichloroethane (TCA) over model sulfated Pt(111) surfaces has been investigated by fast X-ray photoelectron spectroscopy and mass spectrometry. TCA adsorbs molecularly over SO_4 precovered Pt(111) at 100 K, with a saturation coverage of 0.4 monolayer (ML) comparable to that on the bare surface. Surface crowding perturbs both TCA and SO_4 species within the mixed adlayer, evidenced by strong, coverage-dependent C 1s and Cl and S 2p core-level shifts. TCA undergoes complete dechlorination above 170 K, accompanied by C−C bond cleavage to form surface CH_3, CO, and Cl moieties. These in turn react between 170 and 350 K to evolve gaseous CO_2, C_2H_6, and H_2O. Subsequent CH_3 dehydrogenation and combustion occurs between 350 and 450 K, again liberating CO_2 and water. Combustion is accompanied by SO_4 reduction, with the coincident evolution of gas phase SO_2 and CO_2 suggesting the formation of a CO−SO_x surface complex. Reactively formed HCl desorbs in a single state at 400 K. Only trace (<0.06 ML) residual atomic carbon and chlorine remain on the surface by 500 K.

1. Introduction

Platinum-catalyzed hydrocarbon transformations play an important role in both chemical synthesis, within the petrochemical, fine, and pharmaceutical chemicals sectors, and pollution abatement notably for automotive exhaust emission control.[1−3] Fundamental mechanistic insight derived from studies of bare and promoted transition metal surfaces is now aiding the design of next generation heterogeneous catalysts.[4−7] The surface chemistry of halogenated hydrocarbons with transition metal surfaces has attracted much recent interest and has been the subject of review.[8] The low-temperature catalytic destruction of halogenated alkanes is of particular importance for controlling the emission of compounds that deplete ozone in the stratosphere—notably chlorofluorocarbons (CFCs), halons, carbon tetrachloride, and 1,1,1-trichloroethane (TCA) which are tightly regulated under the 1987 Montreal Protocol.[9]

Over single crystal surfaces the reactivity of haloalkanes generally increases from F < Cl < Br < I, with the thermodynamic stability of the metal−halogen bond driving trends in reactivity across the periodic table.[8] Thermal cleavage of the C−I bond is facile, and as a result iodoalkanes are widely employed as precursors to alkyl intermediates with a range of molecular transformations including dehydrogenation, coupling, and oxidation reactions studied over single crystal surfaces. The thermal chemistry of chloroalkanes is less expansive with nondissociative adsorption commonly reported. While the desorption temperature for the molecular state increases with hydrocarbon chain length over Pd(111)[10] and Cu(100)[11] a corresponding increase in the degree of dissociation is only observed for alkyl chain lengths $>C_4$ and $>C_6$, respectively. This is attributed to the longer chain chloroalkane residing on the surface a higher temperatures where they can react. Molecular beam studies show that over Ir(110)[12] the dissociation of chlorinated methanes is correlated with the weakened C−Cl bond strength resulting from an increased degree of Cl substitution. The thermal dissociation of C−Cl bonds over Pt surfaces is less widely investigated.[13−16] Chloroethane is reported to adsorb molecularly on Pt(111) at 100 K, forming a highly oriented monolayer via coordination through the Cl atom, and desorbs without decomposition at 172 K.[15] In contrast an X-ray photoelectron spectroscopy (XPS) study by Freyer et al. suggests some C−Cl cleavage occurs at 110 K.[17] Similarly dehalogenation of *cis*-1,2- and *trans*-1,2-dichloroethene (DCE) has been reported above 200 K on Pt(111),[16] although a more recent synchrotron study by Cassuto et al. found both DCE and 1,1,2-trichloroethene (TCE) simply desorbed at 250 K without any reaction.[18] More recently we have reported that above 130 K dehydrochlorination of 1,1,1-trichloroethane is observed via rapid sequential C−Cl bond scission to form a surface alkylidyne intermediate and HCl.[19,20]

TCA has found traditionally widespread application as an industrial solvent. Unfortunately its volatility[21] and long tropospheric lifetimes[22] result in ∼10−15% of TCA releases reaching the stratosphere,[23] enhancing both ozone depletion and global warming. TCA is therefore classified as a significant nonmethane volatile organic compound and, under the 1990 London amendment[9] to the Montreal Protocol, is due to be completely phased out of production and usage by the end of 2005. Routes to efficient TCA destruction are therefore urgently sought. A catalytic decomposition process offering high selectivity toward HCl, CO_2, or ethane is desired with minimal Cl_2 formation. The conversion of haloalkanes to useful products can also been achieved using Pd/Ag, Pd/Cu,[24] and Pt/Sn[25] bimetallics where higher selectivity to alkenes is observed with increasing Ag, Cu, or Sn content. TCA hydrodechlorination has also been investigated over Pt dispersed on various forms of alumina[26] (though strangely not γ-Al_2O_3). While these catalysts are efficient for complete TCA destruction, there are problems associated with both their selectivity (byproducts including other undesirable haloalkanes such as 1,1-dichloroethylene and 1,1-dichloroethane) and deactivation. The latter is attributed to the strong adsorption of hydrocarbon reaction intermediates and irreversible coke deposition;[27] HCl is not believed to play a

* To whom correspondence may be addressed. E-mail: afl2@york.ac.uk. Tel: +44 1904 434470. Fax: +44 1904 432516.

10.1021/jp054658g CCC: $33.50
Published on Web 12/16/2005

significant role in catalyst self-poisoning. We have recently shown that there is a delicate balance between low-temperature poisoning by accumulated surface chlorine and high-temperature coking over a model Pt(111) catalyst,[19] which also extends to practical dispersed Pt/γ-Al_2O_3 catalysts.[20]

Previously we have demonstrated the efficacy of SO_4 in facilitating low-temperature C−H activation for promotion of propane oxidation over Pt(111)[28] and C_1−C_3 alkane combustion over Pt/Al_2O_3 catalysts[29] More recently we have also shown that a mutual perturbation between SO_4 species and adsorbed alkenes exists on Pt(111)[30,31] surfaces which results in low-temperature CO_2 formation via an alkyl sulfate-like intermediate. The interaction between SO_4/Pt(111) with functional alkanes, namely, chloroalkanes, has not been reported, and it is of interest to determine whether analogous promotional effects can be observed which would benefit the development of new catalyst systems for low-temperature haloalkane destruction.

Here we report a temperature-programmed desorption (TPD) and fast XPS study of the surface chemistry of TCA over sulfated Pt(111). Fast XPS has been employed to obtain quantitative measurements on the surface chemistry of TCA in real time and allow the direct determination of surface reaction pathways for both molecular and atomic surface species. Our findings have been correlated with corresponding TPD measurements where we demonstrate the efficient low temperature (<400 K) destruction of TCA to exclusively CO_2, H_2O, ethane, and HCl.

2. Experimental Section

XPS measurements were carried out at the SuperESCA beamline of the ELETTRA synchrotron radiation source using a Pt(111) single-crystal sample prepared by standard procedures and maintained under ultrahigh vacuum ($\sim 1 \times 10^{-10}$ Torr). Quoted exposures are given in langmuirs (1 langmuir = 1×10^{-6} Torr s^{-1}) and are uncorrected for ion-gauge sensitivity. The crystal was held at 90 K during dosing. 1,1,1-Trichloroethane (Aldrich 99%) was first purified by repeated freeze−pump−thaw cycles prior to background dosing.

C 1s, Cl, and S 2p X-ray photoelectron (XP) spectra were acquired at a photon energy of 400 eV and energy referenced to the Fermi level. The limiting spectral resolution was ~150 meV. Individual spectra were acquired approximately every 30 s during fast XP measurements and Shirley background subtracted over the entire elemental region. Temperature-programmed XP spectra were acquired by application of a linear heating ramp (~0.4 K s^{-1}) to the exposed sample. A common line shape derived from graphitic carbon was adopted for all C 1s components, based on a Doniach−Sunjic profile convoluted with a Gaussian/Lorentzian (4:1) mix with fwhm = 1.1 eV and asymmetry index = 0.062. A similar line shape gave good fits and was employed for all Cl and S components with common fwhm = 0.74/0.61 eV (Cl/S) and asymmetry factor = 0.051/0.115 (Cl/S). Fitting was performed using CASAXPS Version 2.0.35 using the minimum number of peaks required to minimize the *R* factor. Coverages are defined in terms of monolayers (adsorbates/surface Pt atom) with 1 ML = 1.5×10^{15} atoms cm^{-2}. Absolute carbon coverages were determined by calibration with CO. Temperature-programmed reaction spectra were acquired in a separate ultrahigh vacuum system using a VG 300 amu quadrupole mass spectrometer with a heating rate of ~12 K s^{-1}; spectra are uncorrected for ionization cross section. Temperatures were measured from a thermocouple spot-welded to the edge of the Pt(111) sample.

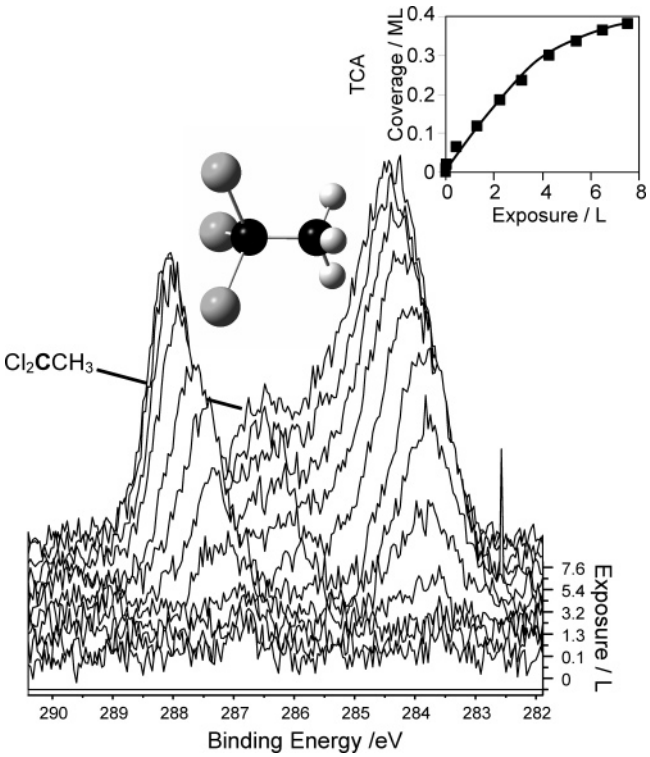

Figure 1. C 1s XP spectra during TCA adsorption onto sulfate presaturated Pt(111) at 95 K. Inset shows integrated surface carbon coverage as a function of TCA exposure.

3. Results and Discussion

3.1. CH_3CCl_3 Adsorption over Sulfated Pt(111). A saturation, pre-sulfated Pt(111) surface was prepared via the sequential coadsorption of O_2 and SO_2 and thermal processing as described elsewhere,[31] resulting in a disordered SO_4 adlayer with $\theta(SO_4)$ = 0.25 ML. Low-temperature TCA adsorption was followed over this surface at 95 K by C 1s fast XPS (Figure 1). At this temperature CH_3CCl_3 adsorbs molecularly over clean Pt(111) giving rise to a well-defined monolayer species, characterized by two well-resolved C 1s peaks at 284.6 and 288.1 eV. These states correspond to the respective $-CH_3$ and $-CCl_3$ chemical functions. Figure 1 reveals that TCA adsorption was largely unperturbed by the presence of preadsorbed sulfate, with both $-CH_3$ and $-CCl_3$ groups clearly resolved ~95 K. However, even at this low temperature a small fraction of the adsorbed TCA underwent partial dechlorination, notably at higher coverages (prolonged exposure), resulting in a small peak around 286 eV attributable to surface CH_3CCl_2 moeities.[19] Illustrative deconvoluted spectra and fits are shown in the Supporting Information (Figure 1S). This latter observation supports an adsorption geometry akin to that on clean Pt(111)[19] wherein reflection/absorption infrared spectroscopy measurements (Supporting Information in ref 19) suggest the methyl group projects away from the surface, with TCA binding through all three Cl atoms allowing facile C−Cl activation.

The saturation TCA coverage was ~0.4 ML (achieved >7 langmuirs exposure) over the pre-sulfated Pt(111) surface, unchanged from that over bare platinum, suggesting negligible site blocking by the preadsorbed SO_4 groups, and consistent with a tightly packed adlayer. Indeed TCA adsorption within the monolayer increased roughly linearly with exposure up to saturation (Figure 1 inset), indicative of precursor-mediated kinetics. Support for such a crowded surface and associated lateral interactions is evinced by the progressive shift of the C 1s components to higher binding energy (BE) with increasing

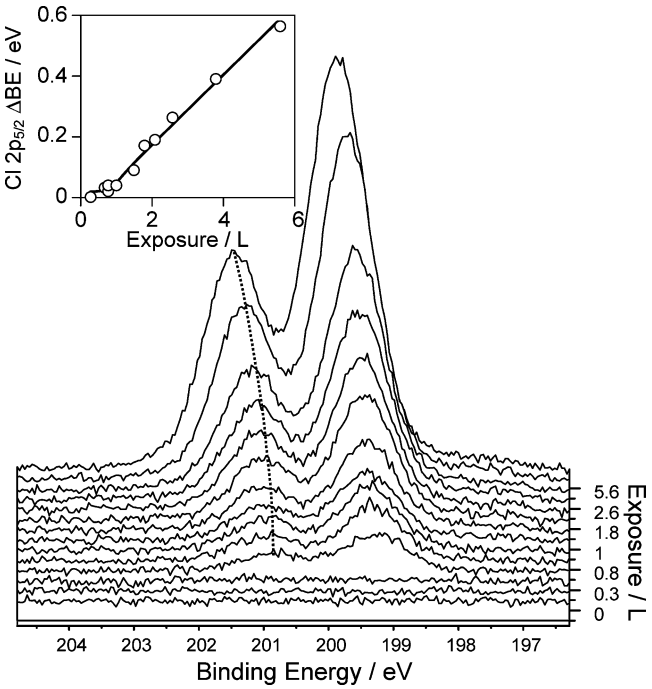

Figure 2. Cl 2p XP spectra during TCA adsorption onto sulfate presaturated Pt(111) at 95 K. Inset shows the shift in Cl $2p_{5/2}$ binding energy with TCA exposure.

TCA coverages above ~0.1 ML (ΔBE = +0.8 eV overall). The presence of strong repulsive lateral interactions is only to be expected in view of the final high density of electronegative coadsorbates present (θ_{Sa} = 0.25 ML, θ_{Cla} = 1.2 ML).

The corresponding Cl 2p fast XP spectra shown in Figure 2 confirm predominantly molecular adsorption, with a chlorine $2p_{3/2}$ component present at 199.9 eV (spin−orbit splitting of 1.56 eV) for saturation TCA as observed over bare Pt(111). The absence of a low binding energy atomic chlorine state ~197.4 eV confirms that only limited, partial TCA dechlorination occurs upon adsorption. It is interesting to note that the Cl 2p core levels show a similar coverage-dependent binding energy shift (ΔBE ~ +0.6 eV overall) as the TCA monolayer builds up. Since both carbon and chlorine core levels move in the same direction by a similar magnitude, it seems more likely that these shifts reflect weaker TCA binding to the Pt(111) substrate on the crowded surface and thus enhanced core−hole lifetimes, i.e., a final-state effect, than their proximity to electron-withdrawing SO_4 groups and thus an initial-state effect.

Comparative S 2p XP spectra shown in Figure 3, demonstrate that the preadsorbed surface sulfate was likewise perturbed upon CH_3CCl_3 adsorption. The well-defined SO_4 doublet at 166.9 eV (S $2p_{5/2}$) on the clean Pt(111) surface is replaced by a much broader, poorly resolved sulfur feature which extends to higher binding energy. This mutual perturbation suggests that TCA and SO_4 form a mixed adlayer facilitating both significant electronic modification and, as discussed later, distinct chemical behavior compared with that of unsulfated platinum. Deconvolution of this perturbed sulfur spectrum was undertaken, using the minimum number of identical doublets with common line shapes, peak widths, and spin−orbit splittings (ΔBE = 1.2 eV), and revealed the presence of two new, high oxidation state (sulfoxy) species at 167.5 and 168.3 eV, which account for ~60% of the total surface sulfur. There are a number of possible scenarios that could account for these new species in the presence of coadsorbed TCA: a change in SO_4 adsorption geometry; indirect electronic perturbation of SO_4 by surface chlorine; or formation of an entirely new surface compound

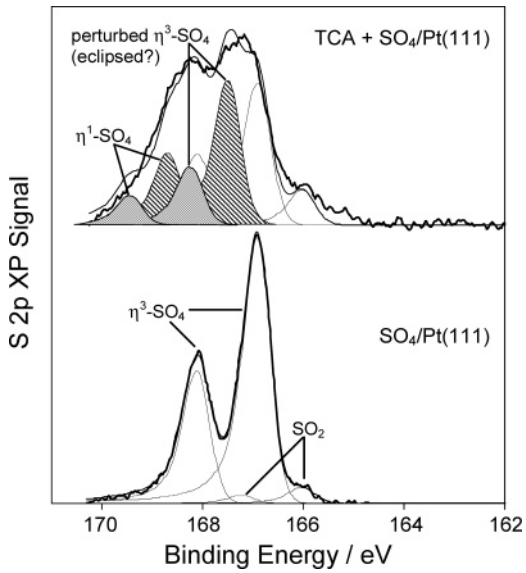

Figure 3. Comparison S 2p XP spectra for a saturation SO_4 adlayer on Pt(111) at 95 K before and after adsorbing a saturation TCA monolayer. New chemical states arising upon TCAadsorption are shaded to aid identification.

such as a thionyl chloride (O=S−Cl_2) derivative. While we cannot entirely discount the latter two possibilities, neither the C 1s or Cl 2p spectra reveal significant TCA dechlorination at 95 K (less than 30% undergoing partial dechlorination to the dichloro- intermediate). It seems improbable that either the amount of free surface chlorine or activation barriers to S−O cleavage are appropriate to facilitate $SOCl_2$ formation at this temperature, and in any event sulfoxy chloride compounds were not observed to desorb upon heating. Sulfate exhibits a number of coordination geometries on both metal and metal oxide surfaces ranging from monodentate (η^1) to tridentate (η^3), with ab initio calculations by Sellers and co-workers identifying the noneclipsed, η^3-mode bound through three oxygens (C_{3v} symmetry) as the preferred geometry over both Ag(111) and Au(111) clusters.[32,33] Steric crowding, such as we suggest occurs when TCA is coadsorbed on SO_4/Pt(111), is expected to weakened the metal−sulfate bond and may force sulfate to adopt the less favored eclipsed or even monodentate geometries. These cluster calculations also reveal that switchovers, from either noneclipsed (η^3) → eclipsed (η^3) or tridentate → monodentate coordinations, should be accompanied by a decrease in the sulfur atom charge density and corresponding increase in the S 2p binding energy.[32] This is consistent with appearance of the new high BE states in Figure 3. We therefore tentatively associate the perturbed sulfoxy species in the coadsorbed TCA + SO_4 adlayer to eclipsed tridentate and/or monodentate sulfate groups.

3.2. CH_3CCl_3 Destruction over Sulfated Pt(111). The thermal chemistry of TCA was subsequently explored over sulfated Pt(111). Figure 4 shows the resulting temperature-programmed C 1s fast XP spectra during heating of a saturation TCA monolayer adsorbed onto a SO_4/Pt(111) surface at 95 K. Characteristic TCA features were lost rapidly upon annealing, reflecting some molecular desorption, coupled with rapid, progressive C−Cl bond scission of the remaining monolayer above 150 K, resulting in disappearance of the 288.1 eV (−CCl_3) and 286.5 eV (−CCl_2) states (see Supporting Information in ref 19 for assignments).

Although rapid, sequential dechlorination also occurs over clean Pt(111), Figure 5 shows clear differences in the fate of the remaining surface carbon species. In the absence of coadsorbed sulfate, TCA dechlorination results in the formation

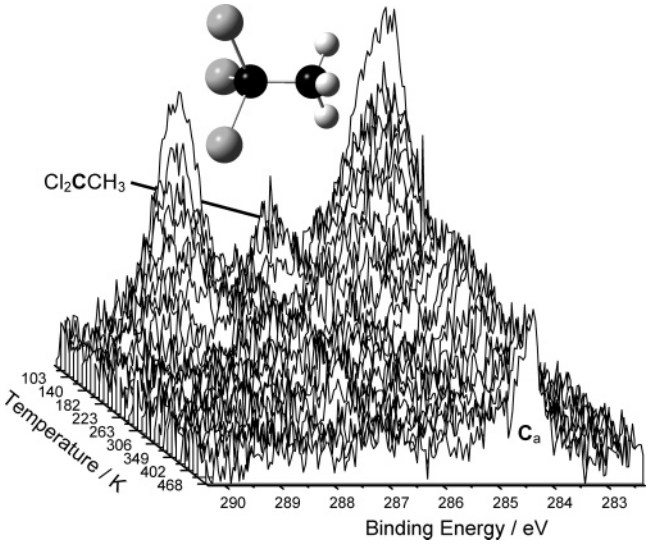

Figure 4. Temperature-programmed C 1s fast XP spectra of a reacting saturated TCA adlayer adsorbed over SO_4/Pt(111) at 95 K.

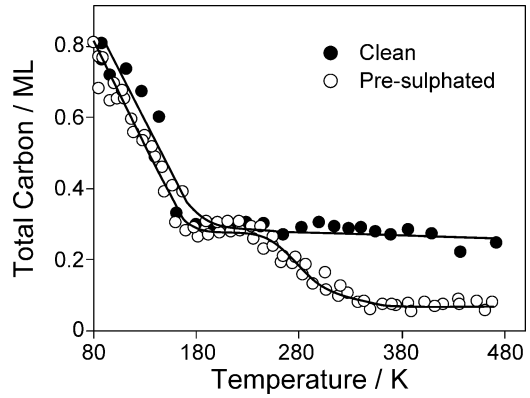

Figure 5. Integrated carbon coverages of reacting saturated TCA adlayers over clean and sulfated Pt(111) surfaces as a function of reaction temperature.

of a stable ethylidyne intermediate ($H_3C-C\equiv$) which in turn dehydrogenates above 350 K depositing substantial (~0.25 ML) irreversibly bound surface carbon. Sulfate clearly modifies the surface chemistry of TCA, with some of the surface hydrocarbon intermediates formed via C−Cl activation desorbing above 220 K. Indeed only trace (<0.06 ML) surface carbon remained above 400 K. This lower residual surface carbon has important implications for the steady-state operation of practical, high area Pt/Al_2O_3 dehydrochlorination catalysts and their deactivation.

The associated Cl 2p spectra, shown in Figure 6, verify that significant low-temperature molecular TCA desorption occurs in the presence of sulfate. At low temperatures the total surface carbon and chlorine signals decrease linearly reflecting molecular TCA desorption which was complete by 200 K. Around 0.33 ML of chlorine persists on the surface above this temperature, present as low binding energy atomic chlorine. This atomic chlorine is rapidly lost above 350 K to leave only 0.05 ML of residual surface chlorine by 500 K.

Evidence that this modified TCA surface chemistry originates from a direct interaction with coadsorbed SO_4 groups, and not for example from simple steric effects within the crowded mixed adlayer, is provided by the temperature-dependent S 2p XP spectra shown in Figure 7. As TCA undergoes dechlorination >180 K, surface sulfate is progressively reduced first to SO_2 and ultimately to atomic sulfur. The total sulfur coverage shows a concomitant decrease, falling from 0.25 to 0.1 ML by room-

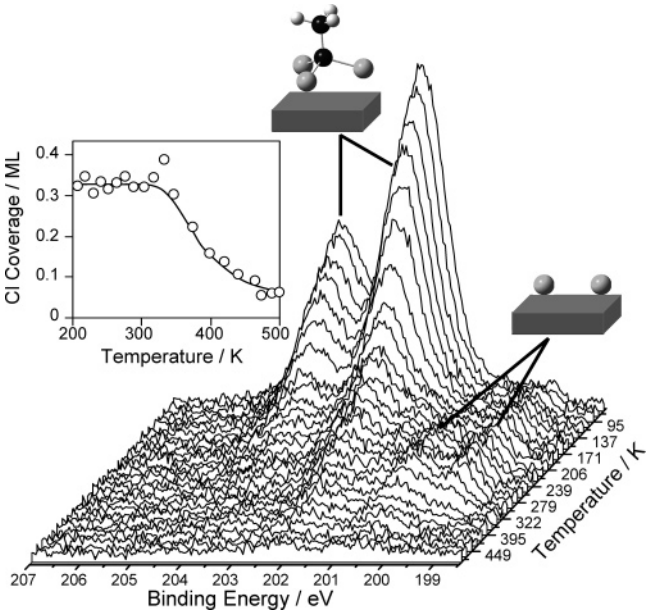

Figure 6. Temperature-programmed Cl 2p fast XP spectra of a reacting saturated TCA adlayer adsorbed over SO_4/Pt(111) at 95 K. Inset shows integrated Cl coverage as a function of reaction temperature.

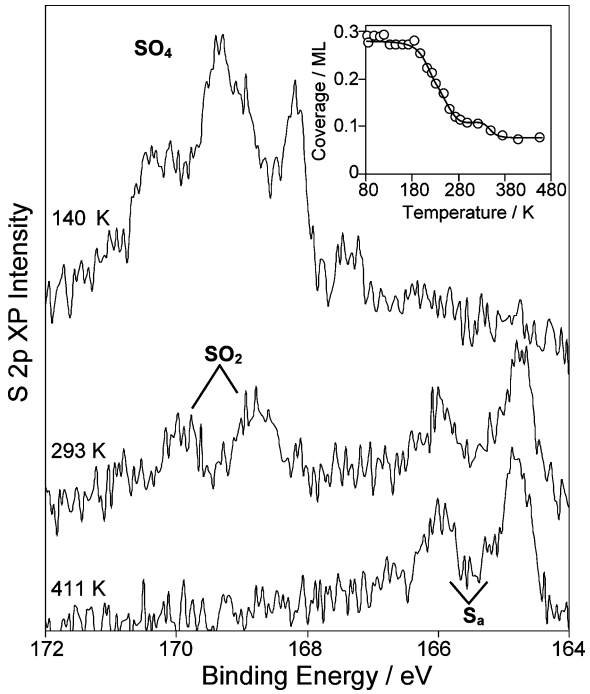

Figure 7. Snapshot S 2p XP spectra from a reacting saturated TCA adlayer adsorbed over SO_4/Pt(111) at 95 K. Inset shows integrated sulfur coverage as a function of reaction temperature.

temperature. These changes cannot be attributed to sulfate decomposition, since SO_4 is thermally stable up to 350 K over clean Pt(111)[31] and must arise from chemical reduction by surface intermediates formed from TCA dechlorination. A further smaller loss of sulfur occurs above 350 K, leaving only ~0.07 ML of atomic sulfur by 480 K.

A more detailed analysis of the C 1s XP spectra in Figure 4 offers additional insight into the nature of the surface intermediates following chlorine abstraction from TCA. Figure 8 compares the carbon environments present on clean and presulfated Pt(111) following warming a saturation TCA adlayer to 300 K. Over bare platinum, ethylidyne formation ensues following C−Cl scission; the C 1s spectrum of a pure ethylidyne adlayer

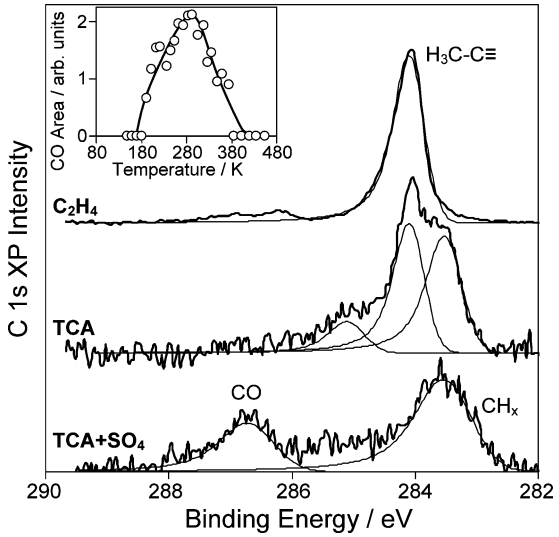

Figure 8. C 1s spectra of saturation TCA adlayers over clean and presulfated Pt(111), and a saturation C_2H_4 monolayer on Pt(111), all adsorbed at 95 K and annealed to 300 K. The integrated CO peak intensity from the TCA + SO_4/Pt(111) annealed surface is shown in the inset.

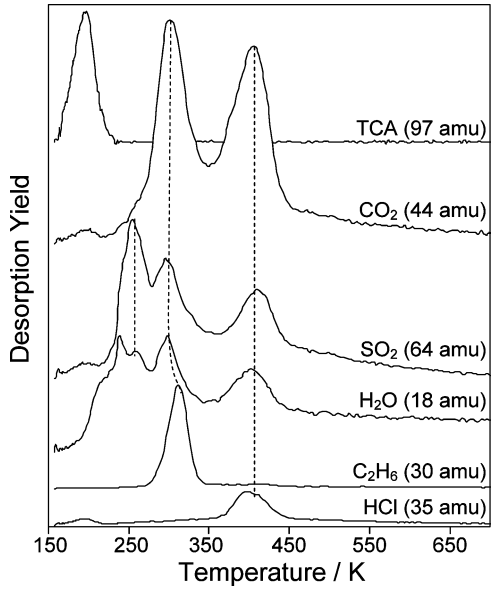

Figure 9. Temperature-programmed desorption spectra for a saturation TCA monolayer adsorbed over a SO_4/Pt(111) surface at 95 K.

on Pt(111), obtained by annealing a saturation C_2H_4 monolayer to 300 K,[30] is shown for comparison. The other significant low binding energy feature at 283.5 eV, which is also observed during the dehydrogenation of ethene to ethylidyne, is tentatively assigned to vinylidene ($H_2C{=}C{=}$). The sharp characteristic ethylidyne feature at 284.1 eV was not observed in the presence of coadsorbed SO_4. In contrast, upon warming the TCA + SO_4/Pt(111) adlayer to room temperature a single, broad low BE state was observed centered around 283.5 eV, together with a high BE feature at 286.7 eV. The low binding energy feature has been observed during the decomposition of both ethene[30] and propene[31] and is attributed to CH_x fragments, while the latter high binding energy state is consistent with that of adsorbed (atop) CO at 287 eV (the Cl 2p spectra show no evidence for carbon−chlorine recombination). Peak fitting reveals the amount of this reactively formed CO increases rapidly above 180 K, reaching a maximum around 300 K. No CO remains adsorbed above 450 K.

3.3. Temperature-Programmed Desorption. The fate of reacting TCA over sulfated Pt(111) was also investigated by thermal desorption spectroscopy; over the bare surface only reversibly adsorbed TCA, HCl, and trace hydrogen desorb (see later). A saturation TCA monolayer was first adsorbed onto a SO_4/Pt(111) surface at 95 K, and thermal desorption products were subsequently monitored by mass spectrometry. Molecular TCA desorbed above 160 K in a single well-defined peak centered at 200 K (Figure 9). A Redhead analysis assuming first-order desorption yielded an activation energy of 48 kJ mol^{-1} for 1,1,1-trichloroethane, in good agreement with its heat of sublimation of around 41 kJ mol^{-1} estimated from ref 34. A variety of reactively formed species desorbed at higher temperatures, and may be generally classified as either combustion or hydrogenation reaction products. Coincident water and SO_2 desorption first occurred around 250 K (note the low-temperature H_2O shoulder arises from loss of molecular water adsorbed from the background). This temperature is below that at which SO_4 thermally decomposes to liberate SO_2 over bare Pt(111),[35] suggesting rather the direct chemical reduction of the preadsorbed SO_4. A second coincident H_2O and SO_2 desorption was observed at 300 K, accompanied by a strong CO_2 desorption. Since the only possible source of surface carbon is adsorbed TCA, this reactively formed CO_2 must originate from subambient C−C cleavage and subsequent combustion via oxygen extraction from coexisting surface sulfoxy moeities. Indeed it is evident from the C 1s XP spectra in Figure 8 that surface CO (or possibly a CO_x-SO_x complex) begins to appear immediately following TCA dechlorination; C−Cl cleavage is accompanied by C−O bond formation. We have previously identified a strong interaction between chemisorbed ethene/propene and SO_4 over Pt(111),[30,31] possibly reflecting low temperature (<200 K) alkyl sulfate formation. It seems likely that a similar synergistic bond making/breaking process operates between the surface $CH_3C{\equiv}$ moieties and SO_4 groups promoting C−C scission, hitherto unheard of at such low temperatures on Pt.

It may be anticipated that such dissociation of the carbon−carbon bond following TCA dechlorination would liberate surface methyl fragments, consistent with the fingerprint low binding energy C 1s peak seen in Figure 8. Further support for low-temperature methyl formation is provided by the appearance of a strong C_2H_6 desorption at 320 K, attributable to recombinative desorption of two surface bound methyl fragments.[36,37] Alternative routes to ethane, such as ethylidyne hydrogenation, can be discounted since our fast XP spectra show no evidence for a surface ethylidyne intermediate, and in any event ethylidyne is stable with respect to hydrogenation under ultrahigh vacuum.[38] The 250 and 300 K water desorptions also suggest the direct interaction (and competitive dehydrogenation) of the methyl fragment of TCA with the Pt(111) surface at subambient temperatures.

A second set of coincident desorption peaks, arising from the combustion of residual surface carbon by the remaining adsorbed sulfoxy groups and hydrogenation of residual surface atomic chlorine and oxygen, occur at 400 K. Methyl dehydrogenation over clean Pt is believed to proceed in a stepwise fashion via a metastable methylene intermediate.[39,37] The second CO_2 desorption state may therefore be attributed to the oxidation of atomic carbon produced from methylene dehydrogenation. Surface hydrogen liberated in such a dehydrogenation step would account for simultaneous HCl and H_2O desorption—the latter oxygen extracted during the reduction of SO_x to irreversibly adsorbed atomic sulfur, as shown in Figure 7.

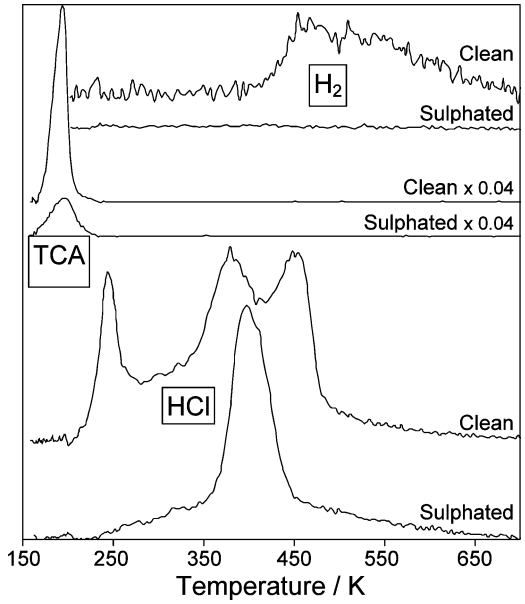

Figure 10. Comparative temperature-programmed desorption spectra from saturated TCA monolayers adsorbed on clean and presulfated Pt(111) at 95 K.

It is interesting that the ratio of the two CO_2 states is almost 1:1—supporting that each is associated with one of the carbons in TCA. The obvious inference is that the low-temperature CO_2 state arises from the $-\mathbf{C}Cl_3$ carbon (the methyl group is still intact at this point accounting for subsequent C_2H_6 evolution), with the 400 K CO_2 desorption resulting from complete dehydrogenation of the H_3C- fragment. The evolution of all these reactively formed products into the gas phase is reaction rate limited, and their appearance is thus indicative of the temperature at which each surface process occurs. The impact of preadsorbed SO_4 on the reactivity of a saturated TCA monolayer over Pt(111) is highlighted in Figure 10. Sulfate increases the reactivity of TCA over platinum, reducing the extent of molecular desorption. TCA combustion by coadsorbed SO_4, and concomitant water formation, mops up any excess hydrogen, eliminating the H−H recombinative desorption seen above 400 K over the clean surface. Sulfation also promotes rapid HCl desorption in a single state ~400 K ($\Delta H_{reax} = 107$ kJ mol^{-1} assuming second order kinetics and $\upsilon = 1 \times 10^{-6}$ molecules^{-1}•m^2•s^{-1}); over bare Pt(111) HCl is formed and evolved in two distinct processes between 300 and 400 K and 400−500 K. The small 240 K HCl desorption from TCA/Pt(111) occurs well below the temperature at which the ethylidyne intermediate dehydrogenates and is associated with Cl clean-off by background adsorbed hydrogen (the $H_a + Cl_a$ reaction can occur as low as 200 K over Pt(111)[40]). The chemistry of TCA over clean and sulfated Pt(111) surfaces is summarized in Scheme 1.

4. Conclusions

The influence of surface sulfate groups on the thermal chemistry of 1,1,1-trichloroethane (TCA) over Pt(111) has been explored by synchrotron fast XPS and therrmal desorption mass spectrometry. TCA adsorbs molecularly at low temperature, without hindrance from the preadsorbed sulfate, and appears to adopt the same adsorption geometry as over bare platinum, binding to the surface through all three chlorines. Lateral interactions within the resulting densely packed mixed adlayer are apparent through strong coverage-dependent binding energy

SCHEME 1. Reaction Pathways of TCA over Clean and Sulfated Pt(111)

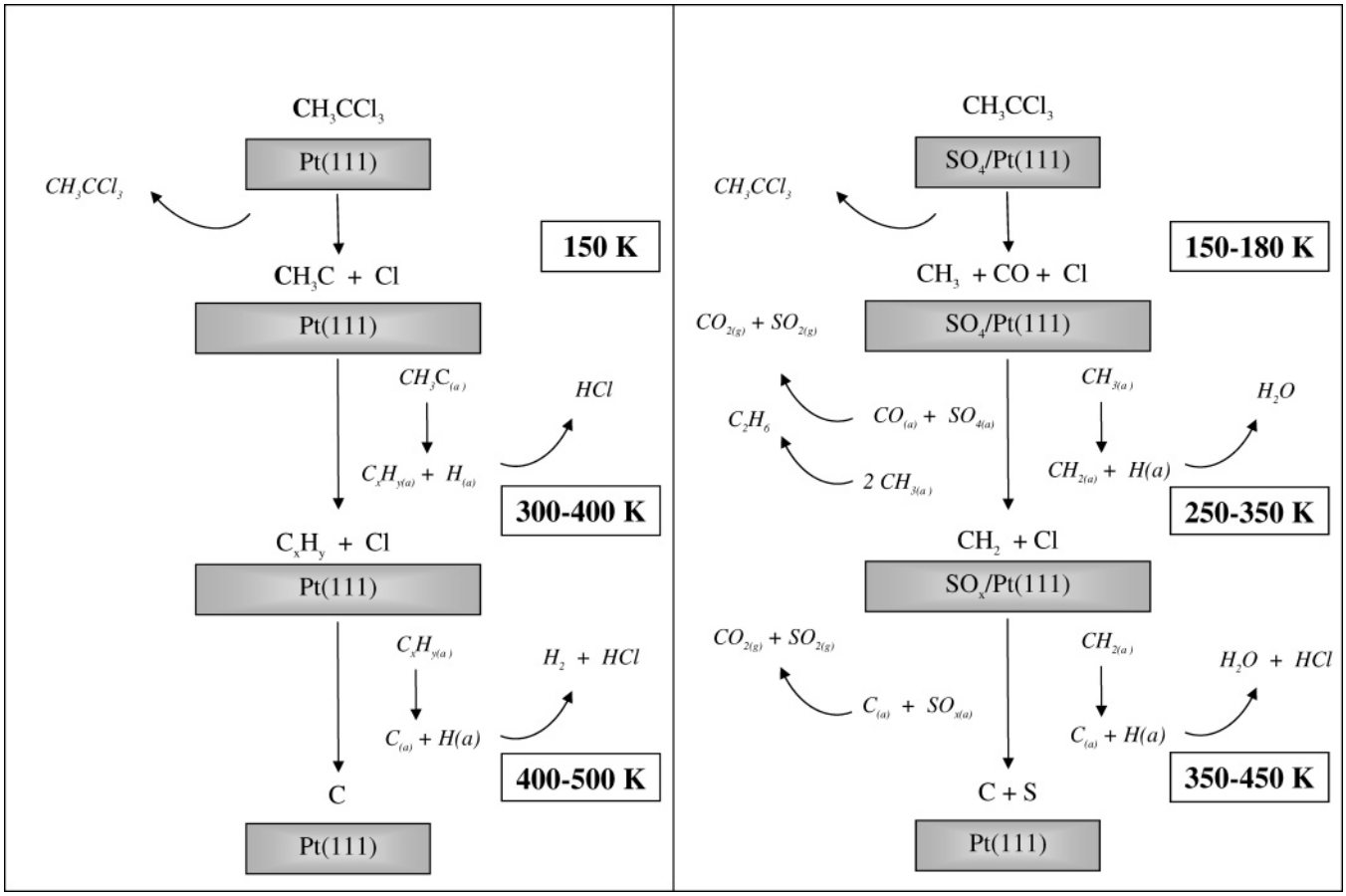

shifts in both C 1s and Cl 2p XP spectra and the associated S 2p XP spectra.

Rapid sequential TCA dechlorination occurs over both clean and presulfated Pt(111) at surface temperatures above 170 K. In the absence of coadsorbed SO_4, the resulting C_2 backbone remains intact and rearranges to form stable ethylidyne (and possibly vinylidene) surface intermediates at room temperature. By contrast, sulfated platinum facilitates C−C dissociation immediately following dechlorination, possibly a result of mutual perturbation or direct complexation of the H_3C-C fragment with SO_4, resulting in low-temperature CO production and simultaneous sulfate reduction. Complete combustion of the initial $-CCl_3$ fragment of TCA yields gas-phase CO_2, sulfur dioxide, and water around 250 K. Above this temperature the CH_3- fragment of TCA follows one of two competing reaction pathways, either recombinative desorption of two methyl groups as ethane, or dehydrogenation and subsequent high-temperature combustion to CO_2 around 400 K. Surface hydrogen liberated during the latter mechanism efficiently removes almost all the atomic chlorine (~0.33 ML) as HCl.

One aspect of this surface chemistry requiring further study is whether surface sulfate acts purely as a chemical promoter opening up alternative reaction pathways or whether it plays a role in site-blocking TCA adsorption, perhaps preventing strong TCA chemisorption on high coordination sites that would normally favor ethylidyne formation. Since the saturation coverage of TCA over clean and SO_4-precovered Pt(111) is the same, the latter possibility does seem unlikely. However TCA adsorption site switching could still be driven by the presence of surface sulfate via strong lateral interactions/electronic pertubation, and we are exploring this possibility. It may prove possible to isolate such chemical/electronic effects from site blocking via addition of an inert bimetal, such as Ag or Au, to generate surface alloys and destroy the critical ensemble for TCA adsorption.

Sulfate therefore appears extremely effective in promoting the complete destruction of a heavily chlorinated (and environmentally unfriendly) hydrocarbon. The reaction products are either benign (CO_2 and H_2O), useful chemical feedstocks (C_2H_6), or readily scrubbed from an effluent stream (SO_2 and HCl). In addition to enhancing the selectivity of platinum-catalyzed TCA destruction, sulfate also helps to minimize undesired surface carbon and chlorine buildup and may thus improve catalyst lifetimes. Clearly for presulfation of Pt/Al_2O_3 catalysts to offer a practical solution to industrial-scale TCA destruction, surface sulfate reduction must be prevented. Oxydechlorination routes, in which oxygen/air is co-fed with TCA vapor, have the potential to overcome this limitation, and we are currently conducting such studies of dispersed $Pt/SO_4-Al_2O_3$ catalysts.

Acknowledgment. We acknowledge support from the European Community—Research Infrastructure Action under the FP6 "Structuring the European Research Area" Program (through the Integrated Infrastructure Initiative "Integrating Activity on Synchrotron and Free Electron Laser Science"), the EPSRC under Grant GRM2087701, and a Royal Society Research Grant 22999. We thank Silvano Lizzit and Andrea Goldoni for assistance with synchrotron measurements.

Supporting Information Available: Deconvoluted C 1s spectra identifying the molecular TCA and dichloroethane components and their associated coverage dependent, integrated peak intensities from Figure 1 are available, together with snapshot Pt 4f spectra of the underlying Pt(111) substrate during SO_4 + TCA adsorption and postreaction. This material is available free of charge via the Internet at http://pubs.acs.org.

References and Notes

(1) Burch, R.; Crittle D. J.; Hayes, M. J. *Catal.* Tod*ay* **1999**, 47, 229.
(2) Garin, F. *Catal. Today* **2004**, *89*, 255.
(3) Davis B. H. *Catal. Today* **1999**, *53*, 443.
(4) Zaera, F. *Surf. Sci.* **2002**, *500*, 947.
(5) Rainer, D. R.; Goodman, D. W. *J. Mol. Catal. A*: *Chem.* **1998**, *131*, 259.
(6) Freund, H. J. *Catal. Today* **2005**, *100*, 3.
(7) Lauritsen, J. V.; Bollinger, M. V.; Laegsgaard, E.; Jacobsen, K. W.; Norskov, J. K.; Clausen, B. S.; Topsoe, H.; Besenbacher, F. *J. Catal.* **2004**, *221*, 510.
(8) Bent, B. E. *Chem. Rev.* **1996**, *96*, 1361.
(9) http://www.unep.org/ozone/index.asp, June 2004.
(10) Zhou, G.; Gellman, A. J. *J. Catal*. **2000**, *194*, 233.
(11) Lin, J−L.; Bent, B. E. *J. Phys. Chem*. **1992**, *96*, 8529.
(12) Reeves, C. T.; Meyer, R. J.; Mullins, C. B. *J. Mol. Catal. A*: *Chem.* **2003**, *202*, 135.
(13) Henderson, M. A.; Mitchell, G. E.; White, J. M. *Surf. Sci. Lett*. **1987**, *248*, L325.
(14) Lloyd, K. G.; Roop, B.; Campion A.; White, J. M. *Surf. Sci*. **1988**, *214*, 227.
(15) Jo, S. K.; Kiss, J.; Polanco, J. A.; White, J. M. *Surf. Sci*. **1991**, *253*, 233.
(16) Hsiao, G. S.; Erley, W.; Ibach, H. *Surf. Sci.* **1998**, *296*, 422.
(17) Freyer, N.; Pirug, G.; Bonzel, H. P. *Surf. Sci*. **1983**, *126*, 487.
(18) Cassuto, A.; Hugenschmidt M. B.; Parent, P.; Laffon, C.; Tourillon, H. G. *Surf. Sci*. **1994**, 310, 390.
(19) Lee, A. F.; Carr, P. A; Wilson, K. *J. Phys. Chem B* **2004**, *108*, 14811.
(20) Lee, A. F.; Carr, P. A.; Wilson, K. *Chem. Commun.* **2004**, 2774.
(21) Midgley, P. M.; Mcculloch A. *Atmos. Environ.* **1995**, *29*, 1601. McCulloch A.; Midgley, P. M. *Atmos. Environ.* **2001**, *35*, 5311.
(22) Derwent, R. G.; Volz-Thomas, A.; Prather, M. J. *World Meteorological Organization Global Ozone Research and Monitoring Project*; Report No. 20; Scientific Assessment of Stratospheric Ozone; WMO: Geneva, Switzerland, 1989; Vol. 2, p 124.
(23) Sidebottom, H.; Franklin, J. *Pure Appl. Chem.* **1996**, *68*, 1757. *World Meteorological Organization, Global Ozone Research and Monitoring Project*; Report No. 20, Scientific Assessment of Stratospheric Ozone, Appendix: AFEAS Report; WMO: Geneva, Switzerland, 1989; Vol. 2, Chapter 6. *World Meteorological Organization, Global Ozone Research and Monitoring Project*; Report No. 25, Scientific Assessment of Stratospheric Ozone Depletion; WMO: Geneva, Switzerland, 1991; Chapter 5.
(24) Lambert, S.; Ferauche, F.; Brasseur, A.; Pirard, J. P.; Heinrichs, B. *Catal. Today* **2005**, *100*, 283.
(25) Rhodes, W. D.; Margitfalvi, J. L.; Borbath, I.; Lazar, K.; Kovalchuk, V. I.; d'Itri, J. L. *J. Catal.* **2005**, *230*, 86.
(26) Frankel, K. A.; Jang, B. W−L..; Spivey, J. J.; Roberts, G. W. *Appl. Catal., A* **2001**, *205*, 263.
(27) Frankel, K. A.; Spivey, J. J.; Roberts, G. W. *Stud. Surf. Sci. Catal.* **2001**, *139*, 439.
(28) Wilson, K.; Hardacre, C.; Lambert, R. M. *J. Phys. Chem.* **1995**, *99*, 13755.
(29) Gawthrope, D. E.; Lee, A. F.; Wilson, K. *Catal. Lett.* **2004**, *94*, 25.
(30) Lee, A. F.; Wilson, K. *J. Vac. Sci. Technol., A* **2003**, *21*, 563.
(31) Lee, A. F.; Wilson, K.; Goldoni, A.; Larciprete, R.; Lizzit, S. *Surf. Sci*. **2002**, *513*, 140.
(32) Patrito, E. M.; Paredes Olivera, P.; Sellers, H. *Surf. Sci.* **1997**, *380*, 264.
(33) Paredes Olivera, P; Patrito, E. M.; Sellers, H. *Surf. Sci.* **1998**, *418*, 376.
(34) NIST Chemistry WebBook, NIST Standard Reference Database Number 69, June 2005 Release.
(35) Wilson, K.; Hardacre, C.; Baddeley, C. J.; Ludecke, J.; Woodruff, D. P.; Lambert, R. M. *Surf. Sci.* **1997**, *372*, 279.
(36) Fairbrother, D. H.; Peng, X. D.; Viswanathan, R.; Stair, P. C.; Trenary, M.; Fan, J. *Surf. Sci.* **1993**, *285*, L455.
(37) Oakes, D. J.; Newell, H. E.; Rutten, F. J. M.; McCoustra, M. R. S.; Chesters, M. A. *J. Vac. Sci. Technol., A* **1996**, *14*, 1439.
(38) Zaera, F.; Janssens, T. V. W; Ofner, H. *Surf. Sci*. **1996**, *368*, 371.
(39) Jenks, C. J.; Bent, B. E.; Zaera, F. *J. Phys. Chem. B* **2000**, *104*, 3017.
(40) Daschbach, J. L.; Kim, J.; Ayotte, P.; Scott Smith, R.; Kay, B. D. *J. Phys. Chem. B* **2005**, *109*, 15506.